

The magnetic structure of cobalt diphosphate $\text{Co}_2\text{P}_2\text{O}_7$

This article has been downloaded from IOPscience. Please scroll down to see the full text article.

1989 J. Phys.: Condens. Matter 1 169

(<http://iopscience.iop.org/0953-8984/1/1/015>)

View [the table of contents for this issue](#), or go to the [journal homepage](#) for more

Download details:

IP Address: 171.66.16.89

The article was downloaded on 10/05/2010 at 15:48

Please note that [terms and conditions apply](#).

The magnetic structure of cobalt diphosphate $\text{Co}_2\text{P}_2\text{O}_7$

J B Forsyth[†], C Wilkinson[‡], S Paster[‡] and B M Wanklyn[§]

[†] Rutherford Appleton Laboratory, Chilton, Oxon OX11 0QX, UK

[‡] Department of Physics, King's College, Strand, London WC2R 2LS, UK

[§] Clarendon Laboratory, University of Oxford, Parks Road, Oxford OX1 3PU, UK

Received 9 August 1988

Abstract. Cobalt diphosphate is shown to become antiferromagnetically ordered below 10.20(5) K and its magnetic structure has been determined from single-crystal unpolarised neutron diffraction measurements at 3.9 K. The structure contains two crystallographically independent Co(II) ions, Co(1) and Co(2), with moments of $3.60(2)\mu_{\text{B}}$ and $3.62(2)\mu_{\text{B}}$, respectively. The magnetic propagation vector is $(\frac{1}{2}00)$ and the magnetic space group is $P_{2a}2_1/c$. The structure is non-collinear with the moments oriented at the spherical polar angles of $\theta = 82.1(2)^\circ$, $\varphi = -0.4(2)^\circ$ and $\theta = 113.5(2)^\circ$, $\varphi = -43.7(2)^\circ$ for Co(1) and Co(2), respectively, the polar axis being parallel to c and φ being measured from the a - c plane. The magnetic form factors of the Co^{2+} ions show a radial expansion with respect to the free ion in excess of that due to their orbital magnetisation. Magnetic coupling within the $(\bar{1}01)$ sheets of Co^{2+} ions includes both direct and super-exchange paths, whereas the coupling between successive sheets must pass through the intervening P_2O_7 groups via Co–O–P–O–Co exchange. The orientations of the moments relative to the single-ion anisotropies and the magnetic exchange paths are discussed.

1. Introduction

Neutron studies of chemical bonding have concentrated on understanding in detail the simpler, relatively ionic salts and oxides and have now made some inroads into chemically more interesting materials such as the phthalocyanines (Figgis *et al* 1981) and bipyridines (Figgis *et al* 1984). Between these extremes, the roles of complex anions such as H_2O , $(\text{CN})^-$ and $(\text{CO}_3)^{2-}$ have also been investigated (Fender *et al* 1986, Figgis *et al* 1985, Brown and Forsyth 1967) but much remains to be done in this domain.

We now report the second of a series of studies of materials containing the tetrahedral complex anion $(\text{PO}_4)^{3-}$, about which little is previously known from neutron measurements. Although the classical polarised neutron diffraction technique has provided the majority of accurate magnetic structure factors on which detailed magnetic models are based, it is often difficult to obtain sufficiently complete sets, owing to the time required for the measurement and the limitations imposed on the type of magnetic structure that can be measured. Some of the obstacles to obtaining data, complete to even a modest value of $(\sin \theta)/\lambda$, are avoided if the integrated intensities of magnetic reflections, rather than polarisation ratios, are measured. This is now practical, since the quality of integrated intensity measurements has improved markedly in recent years

so that accuracies of about 1% are now routinely obtainable. To obtain sufficient precision in magnetic structure factors, an antiferromagnetic structure in which the magnetic and chemical unit cells are different must be chosen, so that the magnetic reflections contain no nuclear scattering. The other limiting consideration is the moment direction. In collinear structures, those Fourier components of the magnetisation whose wavevectors are parallel or nearly parallel to the magnetisation direction cannot be measured accurately, owing to the form of the neutron magnetic interaction vector.

We have already reported the magnetic structure of cobalt orthophosphate ($\text{Co}_3(\text{PO}_4)_2$) which becomes antiferromagnetically ordered below 30 K (Forsyth *et al* 1988). Unfortunately, the quality of the single-crystal sample used in that study was not good enough to yield sufficiently accurate magnetic intensities for a detailed modelling of the non-collinear magnetisation density. We now describe the antiferromagnetic structure of cobalt diphosphate ($\text{Co}_2\text{P}_2\text{O}_7$) which we have determined from unpolarised neutron diffraction measurements on excellent single crystals grown at the Clarendon Laboratory, Oxford. The quality of the diffraction data justifies a more sophisticated magnetic model, which includes the effects of the crystalline field, spin-orbit coupling and covalency, and this will be described in a subsequent paper.

2. Experimental details

The room-temperature crystal structure of $\text{Co}_2\text{P}_2\text{O}_7$ has been determined by Krishnamachari and Calvo (1972) from single-crystal x-ray diffraction measurements. They use the unconventional space group $B2_1/c$ to describe the monoclinic structure, which is isomorphous with that of $\alpha\text{-Mg}_2\text{P}_2\text{O}_7$ (Calvo 1967). We prefer to use the conventional space group $P2_1/c$, since this halves the volume of the unit cell. The cell dimensions

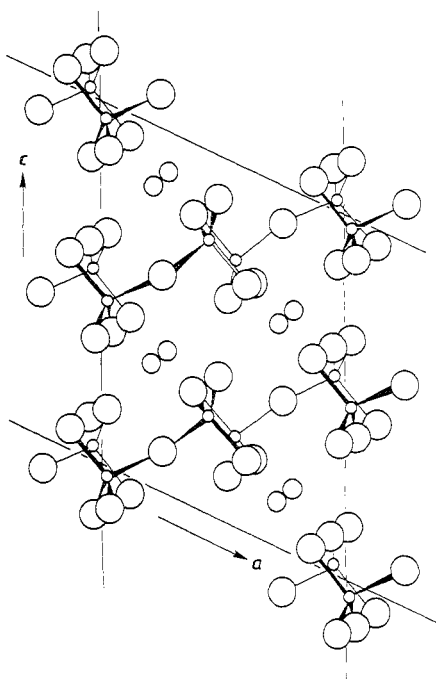


Figure 1. The crystal structure of $\text{Co}_2\text{P}_2\text{O}_7$ referred to the primitive unit cell with $a = 7.008 \text{ \AA}$, $b = 8.345 \text{ \AA}$, $c = 9.004 \text{ \AA}$ and $\beta = 113.84^\circ$. The small full circles represent phosphorus, the large open circles oxygen and the smaller open circles cobalt.

Table 1. The atomic positional parameters in $\text{Co}_2\text{P}_2\text{O}_7$ found by Krishnamachari and Calvo (1972) at room temperature (RT) and in this study at 3.9 K.

Atom	$x(\text{RT})$	$x(3.9 \text{ K})$	$y(\text{RT})$	$y(3.9 \text{ K})$	$z(\text{RT})$	$z(3.9 \text{ K})$
Co(1)	0.2670(1)	0.2684(13)	0.9287(1)	0.9284(15)	0.8906(3)	0.8906(12)
Co(2)	0.2002(1)	0.2004(13)	0.5580(1)	0.5588(13)	0.8254(2)	0.8269(12)
P(1)	0.4404(2)	0.4408(6)	0.2324(3)	0.2319(7)	0.7588(4)	0.7586(6)
P(2)	0.0306(2)	0.0318(6)	0.2257(3)	0.2260(6)	0.4674(4)	0.4665(6)
O(1)	0.2474(4)	0.2490(5)	0.1717(6)	0.1702(6)	0.6001(9)	0.5987(5)
O(2)	-0.1214(5)	-0.1210(5)	0.2353(7)	0.2338(7)	0.5488(11)	0.5496(6)
O(3)	0.6196(5)	0.6196(5)	0.2411(8)	0.2414(14)	0.7033(10)	0.7021(12)
O(4)	0.4750(5)	0.4760(6)	0.0986(7)	0.0992(6)	0.8814(10)	0.8804(5)
O(5)	0.3870(6)	0.3848(7)	0.3900(8)	0.3890(7)	0.8121(12)	0.8093(12)
O(6)	-0.0178(6)	-0.0203(6)	0.0916(7)	0.0909(7)	0.3453(10)	0.3439(5)
O(7)	0.0510(6)	0.0542(6)	0.3861(8)	0.3873(6)	0.3965(12)	0.3984(7)

corresponding to the x-ray study are then

$$a = 7.008(4) \text{ \AA} \quad b = 8.345(3) \text{ \AA} \quad c = 9.004(3) \text{ \AA} \quad \beta = 113.84(6)^\circ.$$

The structure is illustrated in figure 1 and the atomic positional parameters referred to the primitive cell are listed in table 1; the general equivalent positions within the cell are $\pm(x, y, z)$ and $\pm(x, \frac{1}{2} - y, \frac{1}{2} + z)$.

Two single crystals were used in our work and both came from the same batch of samples prepared by flux growth techniques from an initial mixture of CoO , PbF_2 and $\text{NH}_4\text{H}_2\text{PO}_4$ (Wanklyn *et al* 1983). The deep red crystals exhibited a tabular habit, with principal faces $\{110\}$ and elongation parallel to $[2\bar{2}1]$. The magnetic susceptibility of a 62.3 mg crystal was measured parallel to (110) at the Laboratoire Louis Néel, Grenoble. The inverse susceptibility as a function of temperature is illustrated in figure 2 and it clearly shows the onset of antiferromagnetism at 10.1(2) K. The abrupt decrease in the susceptibility below this temperature suggests that a large component of moment must lie near the normal to (110). A distinct change in the slope of the inverse susceptibility with temperature also occurs around 50 K.

The neutron diffraction measurements were made at the Institut Laue-Langevin (ILL), Grenoble, using the D15 diffractometer equipped with an ILL 'Orange' liquid-helium cryostat and a lifting detector, so that integrated intensities could be measured in the normal-beam zero and higher-layer geometry when the sample was oriented with a zone axis approximately vertical. The incident wavelength was 1.174 Å and two crystals, cut to be roughly equiaxed from our second sample, were mounted about $[010]$ and $[001]$. The $[010]$ crystal was first cooled to 4 K and its orientation matrix determined; a search was then made for any reflections with fractional Miller indices whose presence would indicate a commensurate magnetic structure with a cell having dimensions some simple integer multiples of the chemical one. It was quickly established that additional peaks exist with half-integral h -indices, corresponding to a $(\frac{1}{2}00)$ magnetic propagation vector. The temperature dependence of a number of these reflections is shown in figure 3, where it can be seen that they disappear at 10.20(5) K, in good agreement with the transition temperature to paramagnetism found in the susceptibility.

No magnetic intensity corresponding to additional propagation vectors was found and our determination of the magnetic structure successfully accounts for our observations, with magnitudes for the cobalt moments in the range encountered in other neutron studies (3.2–3.8) μ_B .

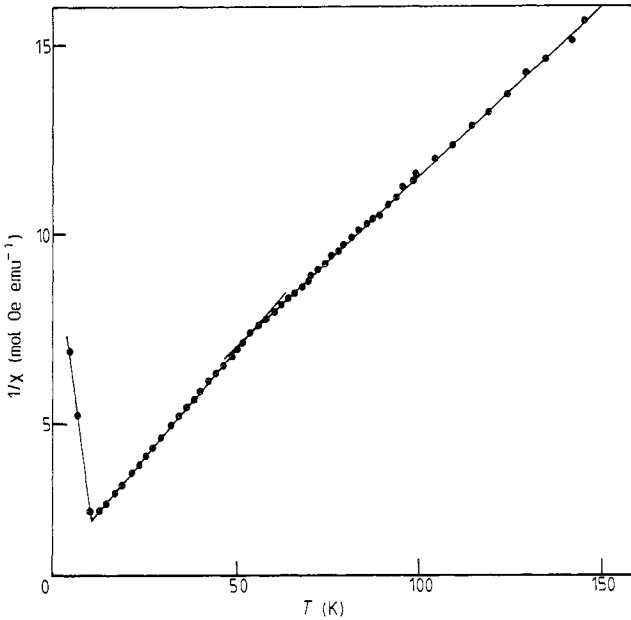


Figure 2. The inverse susceptibility of $\text{Co}_2\text{P}_2\text{O}_7$ as a function of temperature. The Néel point is $10.1(3)$ K.

A total of 841 magnetic reflections were measured with indices $(h + \frac{1}{2}, k, l)$ and $k = 0, 1$ and 2 from the crystal mounted about $[010]$; the equivalents for each reflection were then averaged to produce 445 unique structure factors with $(\sin \theta)/\lambda$ limit of 0.6 \AA^{-1} . A set of 216 $\{0kl\}$ nuclear reflections to a $(\sin \theta)/\lambda$ limit of 0.8 \AA^{-1} was also measured to produce 103 unique structure factors. These were subsequently combined with 100

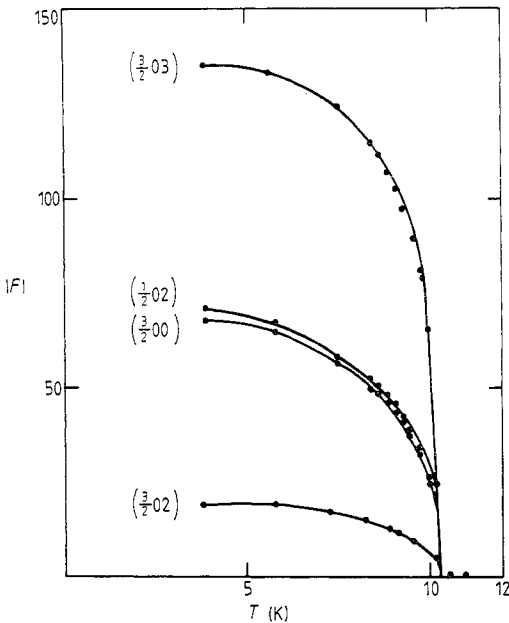


Figure 3. The temperature dependence of a number of magnetic reflections in $\text{Co}_2\text{P}_2\text{O}_7$. They all indicate a Néel point of $10.20(5)$ K.

unique $\{hk0\}$ reflections obtained from 196 integrated intensities from the $[001]$ -oriented sample and used to refine the structure parameters at 3.89 K, to determine absolute scales for the two sets of magnetic reflections and the parameters describing the small amounts of extinction in the samples according to the formalism of Becker and Coppens (1974).

In addition to the $\{hk0\}$ nuclear intensities, the $[001]$ -oriented sample was used to obtain 661 magnetic intensities in the layer lines with $l = 0, 1$ and 2 , which were averaged to produce 313 unique magnetic amplitudes, also to a $(\sin \theta)/\lambda$ limit of 0.6 \AA^{-1} .

Some small intensity was found in reflections with indices $\{h0l\}$ with l odd, which should be systematically absent under the action of the c glide. These intensities were present at 273 K and remained unchanged to 3.89 K. We conclude that they were produced by multiple Bragg scattering and did not result from either a chemical or a magnetic phase transition to a structure with lower chemical symmetry.

Both crystals were measured and their absorption calculated. In no case did the transmission factors differ by more than 3% from a mean value of 0.93.

3. Refinement of the crystal structure at 3.9 K

Table 1 contains the crystal parameters obtained from a least-squares refinement of the combined nuclear reflection data from the two crystals. The temperature factors were constrained to be isotropic to reduce the number of variables and the domain radius was fixed at $50 \times 10^{-6} \text{ m}$. The agreement factor on structure factors was 5.1% and the scale factors for the two crystals were very similar. Extinction amounted to some 33% in the structure factor of the most severely affected reflection.

Table 1 also contains the parameters obtained by Krishnamachari and Calvo (1972) and it can be seen that the positional parameters are essentially the same at the two temperatures. The relatively poor precision in the neutron parameters for the cobalt atoms reflects their weak scattering amplitude, $0.25 \times 10^{-12} \text{ cm}$, relative to oxygen, $0.577 \times 10^{-12} \text{ cm}$.

4. Determination of the magnetic structure at 3.9 K

The magnetic propagation vector $(\frac{1}{2}00)$ implies that the magnetic unit cell is double the chemical one in the a direction and that the moment arrangement within one chemical unit cell is exactly reversed on translation by a . The chemical cell contains two crystallographically inequivalent cobalt atoms in general fourfold positions, each set being formed by the action of the centre of symmetry and the c glide plane.

A significant feature of the magnetic data is the occurrence of reflections of the form $\{h + \frac{1}{2}0l\}$ with l odd, showing that the c glide is not present in the magnetic structure. The magnetic Patterson function approach (Wilkinson 1968, 1973) was used to obtain a trial magnetic structure from which refinement could proceed. Patterson sections were computed from the magnetic data to a limit in $(\sin \theta)/\lambda = 0.4 \text{ \AA}^{-1}$ at heights $y = 0.000, 0.125, 0.375$ and 0.500 , since these contain or lie close to the Co–Co vectors in the structure. Figure 4 illustrates two of these sections and the positions of the Co–Co vectors which they contain. Table 2 gives the positions of the cobalt atoms and table 3 lists the contributions to the Co–Co vectors from the cobalt atoms whose positions are given in table 2. The peak at the origin of the Patterson function corresponds to the sum of the

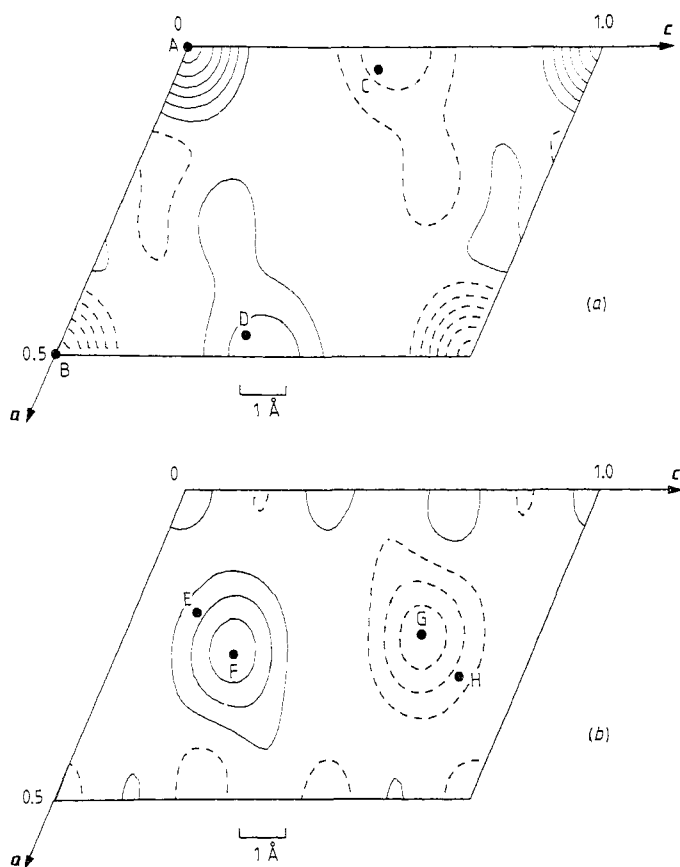


Figure 4. (010) magnetic Patterson sections (a) at $y = 0.0$ and (b) at $y = 0.5$ for $\text{Co}_2\text{P}_2\text{O}_7$. The data are limited to $(\sin \theta)/\lambda \leq 0.4 \text{ \AA}^{-1}$. The positions of the Co-Co vectors contributing to each section are labelled according to the key listed in table 3. Peaks C, D, F and G have some of or all their contributing vectors terminating above and below the section by an amount 0.0133 on y .

squares of the cobalt moments M_1 and M_2 , which were assumed to be equal for the trial structure. A set of simultaneous equations was then derived relating the observed heights of the remaining peaks to the contributing vectors, each of the form $M_1 \cdot M_2$. The solution of these equations was consistent with when the centre of symmetry in the crystal structure was associated with time reversal in the magnetic structure and when

Table 2. The labelling scheme for the cobalt atoms whose Patterson vectors are listed in table 3. Atoms labelled in table 3 as negative (e.g. -A) are related to the unsigned atom (A) by the antiferromagnetic translation a .

Atom label	Transformation		
A	x	y	z
B	$-x$	$-y$	$-z$
C	x	$\frac{1}{2} - y$	$\frac{1}{2} + z$
D	$-x$	$\frac{1}{2} + y$	$\frac{1}{2} - z$

Table 3. Inter-cobalt vectors contributing to the magnetic Patterson function peaks shown in figure 4.

Peak label	Contributing vectors
A ($\equiv -B$)	$(1A)^2 (1B)^2 (1C)^2 (1D)^2 (2A)^2 (2B)^2 (2C)^2 (2D)^2$
C ($\equiv -D$)	$(1C, 2A) (2B, 1D) (1A, 2C) (2D, 1B)$
E ($\equiv -F$)	$(2A, -2D) (2C, -2B)$
G ($\equiv -H$)	$(1A, -2B) (2A, -1B) (1B, 1C) (1D, 1A) (1C, -2D) (2C, -1D)$

the c glide was unchanged. Trial values for the components of magnetisation on the eight cobalt atoms in the chemical cell resulted in an agreement factor on structure factors with $(\sin \theta)/\lambda \geq 0.3 \text{ \AA}^{-1}$ of some 30%, which a least-squares refinement reduced to 8% without extinction correction and 4.7% with this correction included. When this model was used to calculate the fit on the total [010] crystal data to $(\sin \theta)/\lambda = 0.6 \text{ \AA}^{-1}$, however, the agreement rose to 19% and it was evident that the larger-angle data were generally calculated to be smaller than observed.

The magnetic form factor used in the above calculations corresponded to the free-ion wavefunctions calculated for the Co^{2+} ion by Clementi and Roetti (1974), assuming the moment to arise solely from 3d spin. In the dipole approximation to the magnetic form factor of an atom with orbital as well as spin moment, the $2S\langle j_0 \rangle$ radial function is replaced by $2S\langle j_0 \rangle + L\{\langle j_0 \rangle + \langle j_2 \rangle\}$. A refinement in which the $\langle j_2 \rangle$ contribution at each cobalt site was allowed to vary independently, whilst the moment direction was constrained to be the same as that for $\langle j_0 \rangle$, reduced the R -factor to 6.5% and gave values for the $\langle j_0 \rangle$ and $\langle j_2 \rangle$ contributions as follows: for Co(1) the $\langle j_0 \rangle$ contribution was $3.60(2)\mu_B$ and the $\langle j_2 \rangle$ contribution was $1.32(6)\mu_B$; for Co(2) the $\langle j_0 \rangle$ contribution was $3.62(2)\mu_B$ and the $\langle j_2 \rangle$ contribution was $1.32(6)\mu_B$. At no point in the refinement was there any indication that the magnetic structure did not conform to the symmetry deduced from the Patterson maps, namely $P_{2_1}2_1/c$. The final parameters describing the moment directions are as follows: for Co(1), $\theta = 82.1(2)^\circ$ and $\varphi = -0.4(2)^\circ$; for Co(2), $\theta = 113.5(2)^\circ$ and $\varphi = -43.7(2)^\circ$. θ and φ are the polar angles referred to the orthogonal crystal axes with c as the polar axis and φ measured from the a - c plane. The angles were little modified by the inclusion of $\langle j_2 \rangle$ components from those obtained from the small-angle spin-only refinement.

Difference Patterson sections were computed whose coefficients were the arithmetic differences between the observed magnetic intensities and those computed from the best-refined model in an attempt to locate the major sources of difference between the model and the observations. Unfortunately, no meaningful interpretation was possible, in terms of either major asphericities in the magnetisation distribution of the cobalt ions or the moment residing on their oxygen ligands. Further progress in interpreting the residual differences awaits a more detailed description of the Co^{2+} ground-state wavefunction.

5. Discussion

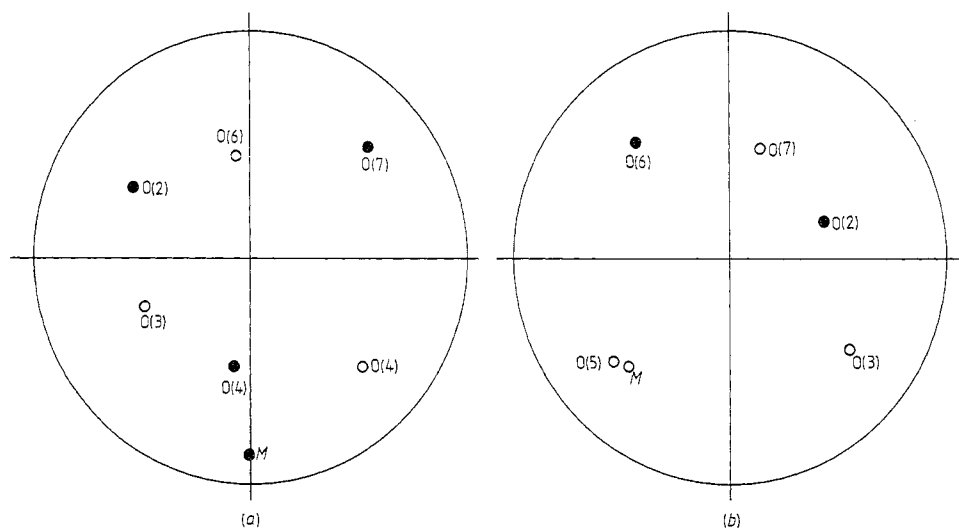
The crystal structure of $\text{Co}_2\text{P}_2\text{O}_7$ (figure 1) is isomorphous with that of the low-temperature β -modification of a number of diphosphates whose high-temperature α -phase has the theortveitite structure (Cruickshank *et al* 1962). The bonding in the α -phases has

Table 4. The bond lengths and angle for the Co–O–Co exchange paths in $\text{Co}_2\text{P}_2\text{O}_7$.

Linkage	Bond lengths (Å)		Angle at oxygen atom (deg)
Co(1)–O(2)–Co(2)	2.099(6)	2.072(6)	98.0
Co(1)–O(3)–Co(2)	2.085(6)	2.067(5)	98.9
Co(1)–O(4)–Co(1')	2.062(7)	2.126(8)	102.5
Co(2)–O(5)–Co(2')	1.957(7)	3.398(12)	100.3
Co(1)–O(6)–Co(2)	2.139(7)	2.040(6)	102.0
Co(1)–O(7)–Co(2)	2.813(7)	2.110(8)	98.7

been well described by Calvo (1967) in his structure determination of $\alpha\text{-Mg}_2\text{P}_2\text{O}_7$. The P_2O_7 groups lie in $(\bar{1}01)$ planes and their terminal oxygen atoms present approximately hexagonally close-packed sheets to the cations which, in the case of Co(1), have irregular octahedral coordination with an average Co–O bond length of 2.10 Å. The Co(2) coordination is generally regarded as being fivefold with an average Co–O bond distance of 2.05 Å; the next-nearest neighbours are O(1), the link oxygen atom of the P_2O_7 group, at a distance of 3.036 Å and two other oxygen atoms, O(6) and O(5), at 3.310 Å and 3.402 Å, respectively.

The shortest paths for direct magnetic exchange between the cobalt ions are confined to contacts within the $(\bar{1}01)$ sandwich between sheets of P_2O_7 groups. The relevant Co–Co distances are as follows: Co(1)–Co(1), 3.281 Å; Co(1)–Co(2), 3.148 and 3.244 Å. Each of the terminal oxygen atoms of the P_2O_7 group is bonded to two cobalt atoms which make an angle at the oxygen atom of between 98 and 102° (table 4); however, the bonds to O(5) include both the shortest and an anomalously long one. Co(1) and Co(2) ions in the same $(\bar{1}01)$ sandwich are linked to each other by four of these bonds and to themselves by one, although, in the case of Co(2)–O(5)–Co(2'), this involves the long 3.4 Å bond.

**Figure 5.** (a) Stereographic projection down $[001]$ showing the orientation of the Co(1) magnetic moment M relative to the coordinating oxygen atoms and (b) the stereogram for Co(2).

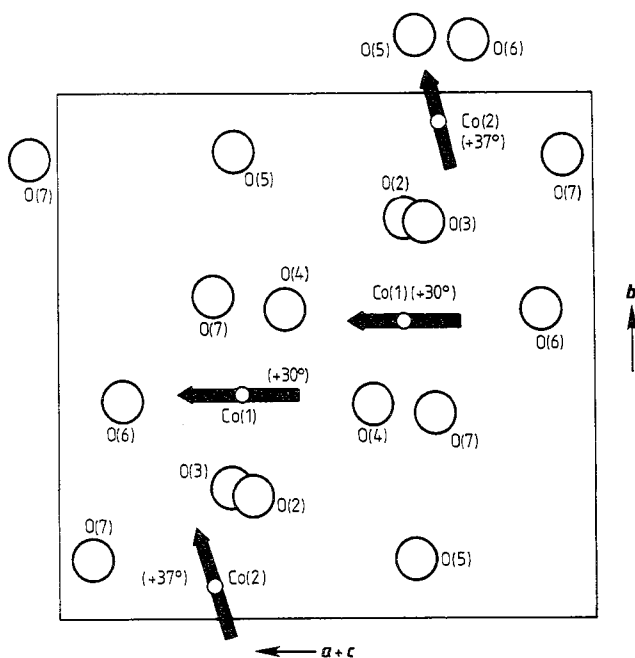


Figure 6. Exchange paths and moment orientations in the $(\bar{1}01)$ planes of cobalt atoms. The projection shows only those oxygen atoms above and below the plane which are bonded to the cobalt atoms. The values in parentheses are the angles of the moments to the plane of projection.

The moment of the Co(1) ion makes an angle of 30° with the $(\bar{1}01)$ sheet in which the cobalt atoms lie and points approximately in the direction of one of the two O(4) atoms forming the superexchange paths to its nearest Co(1) neighbour. The Co(2) moment lies at 37° to the sheet of cobalt atoms and points in the direction of the closest atom O(5) of its fivefold oxygen coordination polyhedron. The moment directions relative to the orientations of the coordinating oxygen atoms are shown in figure 5; figure 6 illustrates the coupling of the moments in the $(\bar{1}01)$ sheets, which is approximately ferromagnetic. Successive $(\bar{1}01)$ sheets (figure 1) are antiferromagnetically coupled.

The magnitudes of the cobalt ion moments and the large contribution of (j_2) to their form factors show that they carry significant orbital magnetisation; we should therefore expect the magnetic structure to be influenced by the single-ion anisotropy resulting from the spin-orbit coupling and, indeed, this is evident from our determination since both moments point at ligand atoms. In the case of the Co(1)–Co(1) neighbours, this is consistent with strict ferromagnetic coupling (figure 6). Between Co(1) and its nearest Co(2) neighbour the coupling is predominantly ferromagnetic with an inter-moment angle of 53° .

The magnitudes of the cobalt moments are very similar, some $3.6(1)\mu_B$, and this is larger than that determined for cobalt salts such as CoF_2 ($3.2(1)\mu_B$). However, in one of the two independent determinations of the non-collinear magnetic structure of β - CoSO_4 , Bertaut *et al* (1963) found a Co^{2+} moment of $3.82(10)\mu_B$ at 4.2 K. This material as a T_N of 12 K, similar to that of $\text{Co}_2\text{P}_2\text{O}_7$, and a structure which again suggests that the local environment is as least as important as magnetic exchange in orienting the moments.

In the parallel investigation, Brown and Frazer (1963) deduced a similar structure, but estimated the Co^{2+} moment to be $3.2(3)\mu_{\text{B}}$. The form factors used in both experiments were different, and the larger error quoted by the latter researchers took into account the rather poor agreement which they obtained between the calculated and observed nuclear structure factors at 77 K, on which the scale of the magnetic scattering depends. In our recent determination of the non-collinear magnetic structure of $\text{Co}_3(\text{PO}_4)_2$ ($T_{\text{N}} = 30\text{K}$), we found moments of $3.77(10)\mu_{\text{B}}$ and $3.49(7)\mu_{\text{B}}$. Taken as a whole, these observations appear consistent with the general hypothesis that the orbital moment of the Co^{2+} ion is less quenched in lower-symmetry environments, leading to a higher total moment and to non-collinear magnetic structures in magnetically dilute salts with their weaker exchange and lower Néel temperatures.

The radial extent of the form factors representing the cobalt ion magnetisations is expanded relative to the spin-only Co^{2+} free-ion factor by more than would be expected from the presence of orbital scattering alone. Although we should expect the moment value to be depressed by the presence of covalency and the zero-point spin deviation, the multipliers of $\langle j_2 \rangle$ are larger than the likely orbital moment; the difference suggests a contraction of the Co^{2+} 3d majority radial wavefunction in the solid relative to the free-ion calculation. The form factor, however, is less expanded than that deduced by Alperin (1961, 1962) from his measurements of Ni^{2+} in NiO. An experimental determination of the g -factors in these materials would enable us to verify our values for their orbital moments.

References

- Alperin H A 1961 *Phys. Rev. Lett.* **6** 55
— 1962 *J. Phys. Soc. Japan Suppl B* **3** 12
Becker P and Coppens P 1974 *Acta Crystallogr. A* **30** 129
Bertaut E F, Coing-Boyat J and Delapalme A 1963 *Phys. Lett.* **3** 178
Brown P J and Forsyth J B 1967 *Proc. Phys. Soc.* **92** 125
Brown P J and Frazer 1963 *Phys. Rev.* **129** 1145
Calvo C 1967 *Acta Crystallogr.* **23** 289
Clementi E and Roetti C 1974 *At. Data Nucl. Data Tables* **14** 177
Cruickshank D W J, Lynton H and Barclay G A 1962 *Acta Crystallogr.* **15** 491
Fender B E F, Figgis B N, Forsyth J B, Reynolds P and Stevens E 1986 *Proc. R. Soc. A* **404** 127
Figgis B N, Forsyth J B and Mason R 1985 *Chem. Phys. Lett.* **115** 454
Figgis B N, Reynolds P A and Mason R 1984 *Inorg. Chem.* **23** 1149
Figgis B N, Williams G A, Forsyth J B and Mason R 1981 *J. Chem. Soc. Dalton Trans.* 1837
Forsyth J B, Wilkinson C, Paster S and Wanklyn B M 1988 *J. Phys. C: Solid State Phys.* **21** 2005
Frazer B C and Brown P J 1962 *Phys. Rev.* **125** 1283
Krishnamachari N and Calvo C 1972 *Acta Crystallogr. B* **28** 2883
Wanklyn B M, Wondre F R, Davidson W and Salmon R 1983 *J. Mater. Sci. Lett.* **2** 511
Wilkinson C 1968 *Phil. Mag.* **17** 609
Wilkinson C 1973 *Acta Crystallogr. A* **29** 449